

Data Repository- Benyon

U-Pb geochronologic analyses of detrital zircon (Nu HR ICPMS)

Zircon crystals are extracted from samples by traditional methods of crushing and grinding, followed by separation with a Wilfley table, heavy liquids, and a Frantz magnetic separator. Samples are processed such that all zircons are retained in the final heavy mineral fraction. A large split of these grains (generally thousands of grains) is incorporated into a 1" epoxy mount together with fragments of our Sri Lanka standard zircon. The mounts are sanded down to a depth of ~20 microns, polished, imaged, and cleaned prior to isotopic analysis.

U-Pb geochronology of zircons is conducted by laser ablation multicollector inductively coupled plasma mass spectrometry (LA-MC-ICPMS) at the Arizona LaserChron Center (Gehrels et al., 2006, 2008). The analyses involve ablation of zircon with a Photon Machines Analyte G2 excimer laser (or, prior to May 2011, a New Wave UP193HE Excimer laser) using a spot diameter of 30 microns. The ablated material is carried in helium into the plasma source of a Nu HR ICPMS, which is equipped with a flight tube of sufficient width that U, Th, and Pb isotopes are measured simultaneously. All measurements are made in static mode, using Faraday detectors with 3×10^{11} ohm resistors for ^{238}U , ^{232}Th , ^{208}Pb - ^{206}Pb , and discrete dynode ion counters for ^{204}Pb and ^{202}Hg . Ion yields are ~0.8 mv per ppm. Each analysis consists of one 15-second integration on peaks with the laser off (for backgrounds), 15 one-second integrations with the laser firing, and a 30 second delay to purge the previous sample and prepare for the next analysis. The ablation pit is ~15 microns in depth.

For each analysis, the errors in determining $^{206}\text{Pb}/^{238}\text{U}$ and $^{206}\text{Pb}/^{204}\text{Pb}$ result in a measurement error of ~1-2% (at 2-sigma level) in the $^{206}\text{Pb}/^{238}\text{U}$ age. The errors in measurement of $^{206}\text{Pb}/^{207}\text{Pb}$ and $^{206}\text{Pb}/^{204}\text{Pb}$ also result in ~1-2% (at 2-sigma level) uncertainty in age for grains that are >1.0 Ga, but are substantially larger for younger grains due to low intensity of the ^{207}Pb signal. For most analyses, the cross-over in precision of $^{206}\text{Pb}/^{238}\text{U}$ and $^{206}\text{Pb}/^{207}\text{Pb}$ ages occurs at ~1.0 Ga.

^{204}Hg interference with ^{204}Pb is accounted for measurement of ^{202}Hg during laser ablation and subtraction of ^{204}Hg according to the natural $^{202}\text{Hg}/^{204}\text{Hg}$ of 4.35. This Hg correction is not significant for most analyses because our Hg backgrounds are low (generally ~150 cps at mass 204).

Common Pb correction is accomplished by using the Hg-corrected ^{204}Pb and assuming an initial Pb composition from Stacey and Kramers (1975). Uncertainties of 1.5 for $^{206}\text{Pb}/^{204}\text{Pb}$ and 0.3 for $^{207}\text{Pb}/^{204}\text{Pb}$ are applied to these compositional values based on the variation in Pb isotopic composition in modern crystal rocks.

Inter-element fractionation of Pb/U is generally ~5%, whereas apparent fractionation of Pb isotopes is generally <0.2%. In-run analysis of fragments of a large zircon crystal (generally every fifth measurement) with known age of 563.5 ± 3.2 Ma (2-sigma error) is used to correct for this fractionation. The uncertainty resulting from the calibration correction is generally 1-2% (2-sigma) for both $^{206}\text{Pb}/^{207}\text{Pb}$ and $^{206}\text{Pb}/^{238}\text{U}$ ages.

Concentrations of U and Th are calibrated relative to our Sri Lanka zircon, which contains ~518 ppm of U and 68 ppm Th.

The resulting interpreted ages are shown on Pb*/U concordia diagrams and relative age-probability diagrams using the routines in Isoplot (Ludwig, 2008). The age-probability diagrams show each age and its uncertainty (for measurement error only) as a normal distribution, and sum all ages from a sample into a single curve.

References:

Gehrels, G.E., Valencia, V., Ruiz, J., 2008, Enhanced precision, accuracy, efficiency, and spatial resolution of U-Pb ages by laser ablation–multicollector–inductively coupled plasma–mass spectrometry: *Geochemistry, Geophysics, Geosystems*, v. 9, Q03017, doi:10.1029/2007GC001805.

Gehrels, G.E., Valencia, V., Pullen, A., 2006, Detrital zircon geochronology by Laser-Ablation Multicollector ICPMS at the Arizona LaserChron Center, in Loszewski, T., and Huff, W., eds., *Geochronology: Emerging Opportunities*, Paleontology Society Short Course: Paleontology Society Papers, v. 11, 10 p.

Ludwig, K.R., 2008, Isoplot 3.60. Berkeley Geochronology Center, Special Publication No. 4, 77 p.

Stacey, J.S., and Kramers, J.D., 1975, Approximation of terrestrial lead isotope evolution by a two-stage model: *Earth and Planetary Science Letters*, v. 26, p. 207-221.

Table with columns for sample ID, U, 206Pb, U/Th, 206Pb*, 235U*, 206Pb*, 238U, error, 206Pb*, 238U*, 207Pb*, 235U, 206Pb*, Best age (Ma), and Conc (%).

5. Location: 1AA/06-18-085-06W4/0

Table with columns for Analysis, U (ppm), 206Pb/204Pb, U/Th, 206Pb*/207Pb* (%), 207Pb* (±), 235U* (±), 206Pb* (±), 238U (±), error (±), 206Pb*/238U* (±), 207Pb* (±), 235U (±), 206Pb*/207Pb* (±), Best age (Ma) (±), and Conc (%).

K-S Test

K-S P-values using error in the CDF

	9	7	8	2	5	3	6	4	1
9		0.060	0.297	0.000	0.000	0.001	0.000	0.303	0.000
7	0.060		0.550	0.000	0.000	0.000	0.000	0.046	0.025
8	0.297	0.550		0.000	0.000	0.000	0.000	0.001	0.046
2	0.000	0.000	0.000		0.435	0.925	0.521	0.027	0.000
5	0.000	0.000	0.000	0.435		0.479	0.249	0.045	0.000
3	0.001	0.000	0.000	0.925	0.479		0.694	0.151	0.000
6	0.000	0.000	0.000	0.521	0.249	0.694		0.052	0.000
4	0.303	0.046	0.001	0.027	0.045	0.151	0.052		0.000
1	0.000	0.025	0.046	0.000	0.000	0.000	0.000	0.000	

K-S P-values for no error

	9	7	8	2	5	3	6	4	1
9		0.048	0.196	0.000	0.000	0.001	0.000	0.239	0.000
7	0.048		0.411	0.000	0.000	0.000	0.000	0.045	0.016
8	0.196	0.411		0.000	0.000	0.000	0.000	0.001	0.034
2	0.000	0.000	0.000		0.278	0.545	0.127	0.018	0.000
5	0.000	0.000	0.000	0.278		0.297	0.151	0.018	0.000
3	0.001	0.000	0.000	0.545	0.297		0.325	0.097	0.000
6	0.000	0.000	0.000	0.127	0.151	0.325		0.040	0.000
4	0.239	0.045	0.001	0.018	0.018	0.097	0.040		0.000
1	0.000	0.016	0.034	0.000	0.000	0.000	0.000	0.000	

Average K-S P-values using Monte-Carlo

	9	7	8	2	5	3	6	4	1
9		0.049	0.178	0.000	0.000	0.001	0.000	0.244	0.000
7	0.049		0.425	0.000	0.000	0.000	0.000	0.037	0.011
8	0.178	0.425		0.000	0.000	0.000	0.000	0.001	0.037
2	0.000	0.000	0.000		0.328	0.703	0.324	0.016	0.000
5	0.000	0.000	0.000	0.328		0.374	0.133	0.022	0.000
3	0.001	0.000	0.000	0.703	0.374		0.417	0.096	0.000
6	0.000	0.000	0.000	0.324	0.133	0.417		0.044	0.000
4	0.244	0.037	0.001	0.016	0.022	0.096	0.044		0.000
1	0.000	0.011	0.037	0.000	0.000	0.000	0.000	0.000	

D-values using error in the CDF

	9	7	8	2	5	3	6	4	1
9		0.189	0.138	0.330	0.299	0.302	0.302	0.141	0.301
7	0.189		0.112	0.377	0.345	0.361	0.382	0.200	0.212
8	0.138	0.112		0.445	0.429	0.435	0.435	0.274	0.194
2	0.330	0.377	0.445		0.126	0.086	0.116	0.213	0.580
5	0.299	0.345	0.429	0.126		0.133	0.148	0.203	0.551
3	0.302	0.361	0.435	0.086	0.133		0.111	0.181	0.568
6	0.302	0.382	0.435	0.116	0.148	0.111		0.197	0.567
4	0.141	0.200	0.274	0.213	0.203	0.181	0.197		0.411
1	0.301	0.212	0.194	0.580	0.551	0.568	0.567	0.411	

D-values for no error

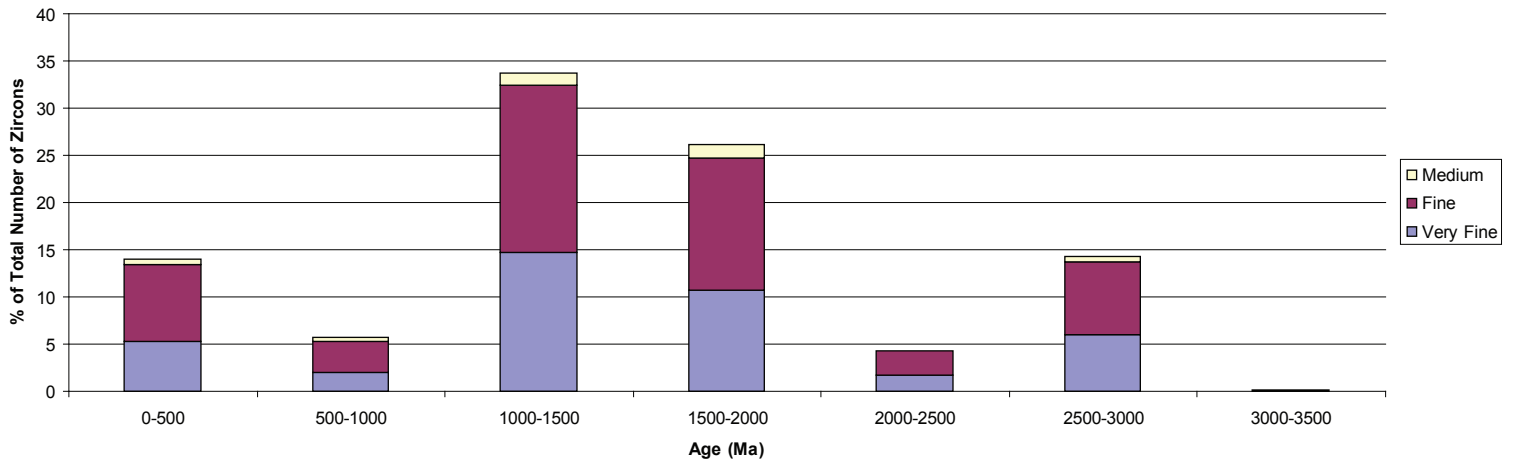
	9	7	8	2	5	3	6	4	1
9		0.195	0.152	0.338	0.309	0.306	0.316	0.150	0.313
7	0.195		0.125	0.384	0.357	0.360	0.393	0.200	0.221
8	0.152	0.125		0.453	0.434	0.439	0.441	0.279	0.202
2	0.338	0.384	0.453		0.143	0.125	0.167	0.223	0.590
5	0.309	0.357	0.434	0.143		0.154	0.165	0.226	0.551
3	0.306	0.360	0.439	0.125	0.154		0.149	0.196	0.576
6	0.316	0.393	0.441	0.167	0.165	0.149		0.203	0.568
4	0.150	0.200	0.279	0.223	0.226	0.196	0.203		0.416
1	0.313	0.221	0.202	0.590	0.551	0.576	0.568	0.416	

Two std devs. of P-values using Monte-Carlo

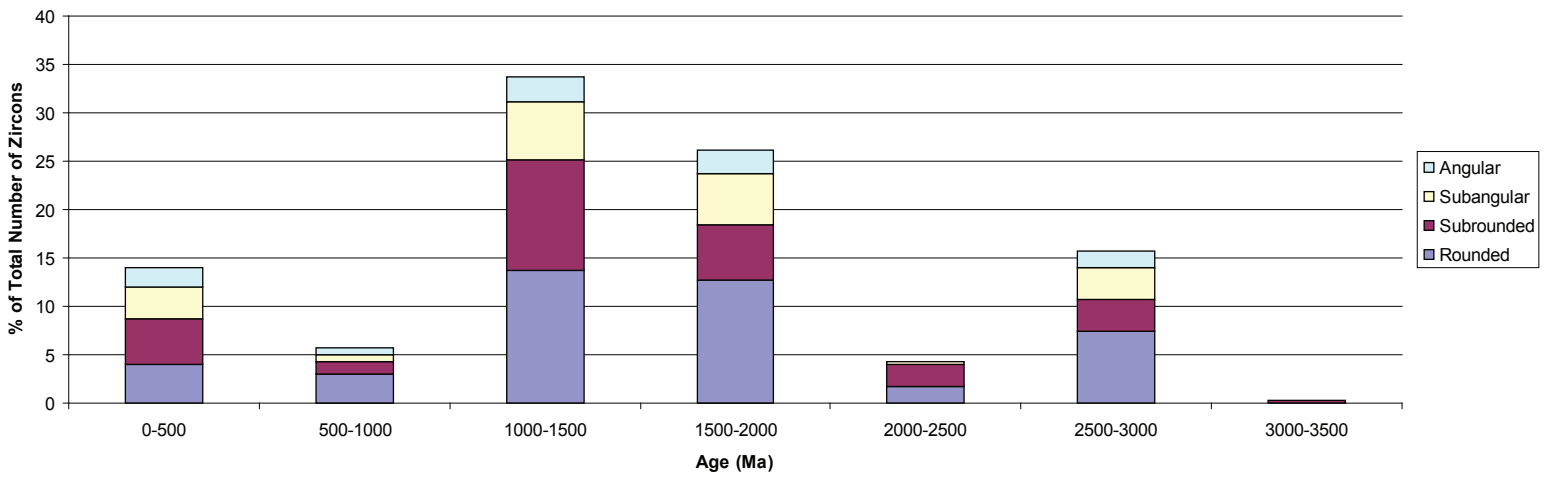
	9	7	8	2	5	3	6	4	1
9		0.012	0.085	0.000	0.000	0.001	0.000	0.059	0.000
7	0.012		0.120	0.000	0.000	0.000	0.000	0.015	0.012
8	0.085	0.120		0.000	0.000	0.000	0.000	0.001	0.022
2	0.000	0.000	0.000		0.214	0.319	0.333	0.016	0.000
5	0.000	0.000	0.000	0.214		0.148	0.098	0.023	0.000
3	0.001	0.000	0.000	0.319	0.148		0.345	0.068	0.000
6	0.000	0.000	0.000	0.333	0.098	0.345		0.014	0.000
4	0.059	0.015	0.001	0.016	0.023	0.068	0.014		0.000
1	0.000	0.012	0.022	0.000	0.000	0.000	0.000	0.000	

Grain Morphology Analysis

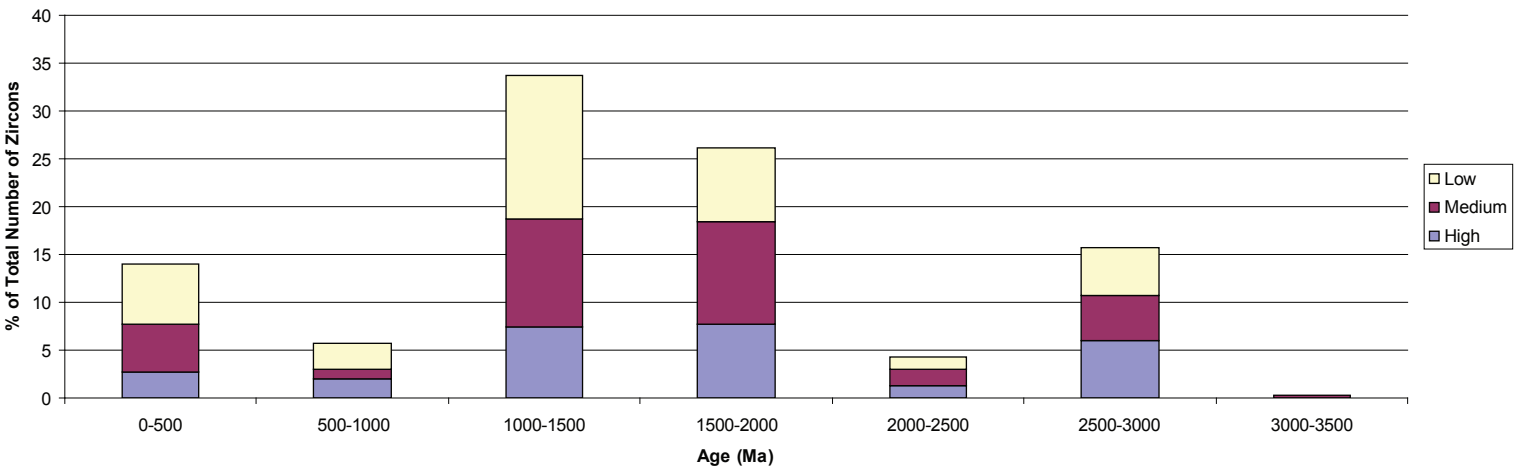
Zircon Grain Size for Samples 1, 2 and 8



Zircon Roundness for Samples 1, 2 and 8



Zircon Sphericity for Samples 1, 2 and 8



Zircon roundness was measured using a comparison to standard frameworks, and sphericity was estimated using a round and elongate grain as endmembers.